VOLUME 27 NUMBER 1

ACCOUNTS OF CHEMICAL RESEARCH®

JANUARY 1994

Registered in U.S. Patent and Trademark Office; Copyright 1994 by the American Chemical Society

On the Difference between Resonance Raman Scattering and Resonance Fluorescence in Molecules: An Experimental View

LAWRENCE D. ZIEGLER

Department of Chemistry, Boston University, Boston, Massachusetts 02215

Received March 29, 1993 (Revised Manuscript Received September 30, 1993)

General Introduction

The characterization of laser excited resonance emission from electronically excited states as either resonance Raman scattering (RRS) or resonance fluorescence (RF) has long been a subject on considerable interest and controversy. Resonance here refers to laser wavelengths which are coincident with electronic absorptions of the material. Determining which of these emission types one is viewing is essential in order to properly extract structural and dynamical information from these observations. Despite the long history and significant number of treatments discussing the characterization of resonance emission as RRS or RF, questions still arise about this tissue. The purpose of this Account is to provide a few simple experimental examples which clearly illustrate those parameters which control the distribution of excited-state energy into these two categories of resonant emissions.

Resonance Emission Definitions. Different types of spontaneous emissions may appear when laser light impinges on a sample, depending upon the excitation wavelength. If this radiation falls in a region of optical transparency, Raman scattering can be observed. The difference between the incident and emitted frequencies corresponds to inelastic ground electronic state transitions, the observed spectral bandwidth is determined by (ro)vibrational relaxation parameters, and the emitted frequency tracks with the incident frequency. However, when the excitation falls in a region of electronic absorption, a more complicated emission spectrum may appear, in general. Some emission features continue to track with the incident light and in all respects are Raman-like (RL), as defined above, while other emission features appear to originate from those excited-state molecular levels resonant with the incident excitation. These features remain fixed in emission frequency as the excitation is tuned in the vicinity of the electronic resonance and correspond to energy level spacings between the excited and ground electronic states. The width of these bands is generally broader than the RL bands and corresponds to electronic relaxation parameters. Such properties describe fluorescence-like (FL) character. These two phenomenologically defined resonance emission components (RL and FL) comprise what we will refer to here as the resonant secondary radiation (RSR) spectrum. This resonance emission is meant to be differentiated from the more common, fully relaxed fluorescence which results from a population equilibrated in all but electronic degrees of freedom with its environment.

Brief Historical Perspective. The resonance emission of diatomic vapors was observed as early as 1906.[1] However, with the advent of tunable laser sources for excitation, the RSR of gases, liquids, and solids could be observed as a function of a larger incident frequency range and under a wider variety of experimental conditions. In the 1970s and early 1980s the assignment of RSR as resonance Raman scattering (RRS) or resonance fluorescence (RF) of some mixture

Lawrence Ziegler is associate Professor of Chemistry at Boston University. He received his B.S. degree from SUNY at Stony Brook in 1971, where he worked with P. M. Johnson, and his Ph.D. at Cornell University in 1978, with A. C. Albrecht. He was an NIH postdoctoral fellow with B. S. Hudson at Stanford and the University of Oregon, and a National Research Council Associate at the Naval Research Lab before joining the chemistry faculty at Northeastern University in 1983. He moved to BU in 1992. His research interests include nonlinear optical spectroscopy and ultrafast dynamics in gas and condensed phases.

(1) Wood, R. W. *Philos. Mag.* **1906**, *12*, 499. Wood, R. W.; Hackett, F. E. *Astrophys. J.* **1909**, *30*, 339.

0001-4842/94/0127-0001$04.50/0 © 1994 American Chemical Society

was the subject of extensive study and controversy.[2-21] Various predicted aspects of the distinction of RSR emission as RRS and RF were critically examined in several experimental studies. These included the analysis of the resonance emission of atomic vapors,[7,13] I_2 vapor,[4] azulene in a naphthalene crystal,[10] and complex biological molecules.[9,11,13] More recent observations of RSR of molecules in solution have been shown to be probes of ultrafast solution dynamics.[22-25]

Theoretical Background. A brief theoretical introduction is necessary in order to appreciate those molecular and experimental parameters that control the partition of RSR into RL and FL features and may also help reveal how some confusion over the use of the RRS vs RF labels has persisted. In general, a quantum statistical density matrix formalism is the most convenient and useful framework for the description of RSR.[3,14-17] This theoretical approach properly captures all of the material relaxation pathways that are *not* included in a simple (second order) perturbation theory (Kramers–Heisenberg) description particularly necessary for condensed-phase systems.[26,27]

For the purposes of this review, we succinctly summarize theoretical expressions (the so-called fast modulation limit of the general stochastic model[16,17]) below for the molecular energy level system pictured in Figure 1. The emission intensity appearing at frequency ν_s due to RSR transitions which originate in level i and terminate in level f of the ground electronic state, excited by monochromatic excitation at ν_l, can be given as the sum of three terms:[14-16]

$$I_{RSR}(\nu_l,\nu_s) = I_{RRS}(\nu_l,\nu_s) + I_{RF}(\nu_l,\nu_s) + I_{mix}(\nu_l,\nu_s) \quad (1)$$

$$I_{RRS}(\nu_l,\nu_s) \propto P_i \left| \sum_e \frac{\langle i|r_l|e\rangle\langle e|r_s^*|f\rangle}{\nu_{ei} - \nu_l + i\Gamma_{ei}} \right|^2 \times \left(\frac{\Gamma_{fi}}{(\nu_{fi} - \nu_l + \nu_s)^2 + \Gamma_{fi}^2} \right) \quad (2)$$

(2) Hizhnykov, V.; Tehver, I. *Phys. Status Solodi* **1967**, *21*, 755.
(3) Shen, Y. R. *Phys. Rev. B* **1974**, 622.
(4) Williams, P. F.; Rousseau, D. L.; Dworetsky, S. H. *Phys. Rev. Lett.* **1974**, *32*, 196. Rousseau, D. L.; Patterson, G. D.; Williams, P. F. *Phys. Rev. Lett.* **1975**, *34*, 1306. Rousseau, D. L.; Williams, P. F. *J. Chem. Phys.* **1976**, *64*, 3519.
(5) Eberly, J. H. *Phys. Rev. Lett.* **1976**, *37*, 1387.
(6) Takagaha, T.; Hanamura, E.; Kubo, R. *J. Phys. Soc.* **1977**, *43*, 802.
(7) Carlsten, J. L.; Szoke, A.; Raymer, M. G. *Phys. Rev. A* **1977**, *15*, 1029.
(8) Cooper, J.; Ballagh, R. J. *Phys. Rev. A* **1978**, *18*, 1302.
(9) Friedman, J. M.; Rousseau, D. L. *Chem. Phys. Lett.* **1978**, *55*, 488.
(10) Hochstrasser, R. M.; Nyi, C. A. *J. Chem. Phys.* **1979**, *70*, 1112.
(11) Friedman, J. M. *J. Chem. Phys.* **1979**, *71*, 3147.
(12) Raymer, M. G.; Carlsten, J. L.; Pichler, G. *J. Phys. B* **1979**, *12*, 119.
(13) Champion, P. M.; Lange, R. *J. Chem. Phys.* **1980**, *73*, 5947.
(14) Fujimura, Y.; Kono, H.; Nakajima, T.; Lin, S. H. *J. Chem. Phys.* **1981**, *75*, 99.
(15) Lee, D.; Albrecht, A. C. In *Advances in Infrared and Raman Spectroscopy*; Clark, R. J. H., Hester, R. E., Eds.; Wiley-Heyden: New York, 1985; Vol. 12, pp 179–213.
(16) Mukamel, S. *J. Chem. Phys.* **1985**, *82*, 5398.
(17) Sue, J.; Jing, Y.; Mukamel, S. *J. Chem. Phys.* **1986**, *85*, 462.
(18) Melinger, J. S.; Albrecht, A. C. *J. Chem. Phys.* **1986**, *84*, 1247.
(19) Melinger, J. S.; Albrecht, A. C. *J. Phys. Chem.* **1987**, *91*, 2704.
(20) Mukamel, S. *Adv. Chem. Phys.* **1988**, *70*, 165; *Annu. Rev. Phys. Chem.* **1990**, *41*, 647.
(21) Shapiro, M. *J. Phys. Chem.* **1993**, *97*, 7396.
(22) Myers, A. B.; Li, B.; Ci, X. *J. Chem. Phys.* **1988**, *89*, 1876.
(23) Myers, A. B.; Li, B. *J. Chem. Phys.* **1990**, *92*, 3310.
(24) Nibbering, E. T. J.; Duppen, K.; Wiersma, D. A. *J. Chem. Phys.* **1990**, *93*, 5477.
(25) Yang, T.-S.; Myers, A. B. *J. Chem. Phys.* **1991**, *95*, 6207.
(26) Yan, Y.; Mukamel, S. *J. Chem. Phys.* **1987**, *86*, 6085.
(27) Sue, J.; Mukamel, S. *Chem. Phys. Lett.* **1984**, *107*, 398.

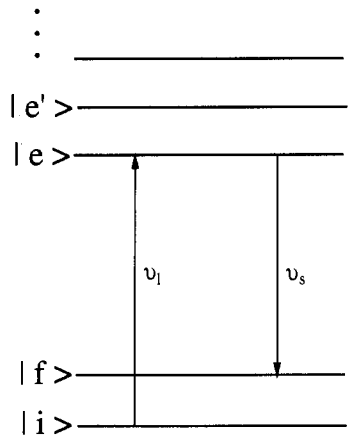

Figure 1. Molecular energy level diagram defining the resonant secondary radiation process: i and f are molecular levels belonging to the ground electronic state; e and e′ are molecular levels belonging to the excited-state manifold; ν_l and ν_s are the incident laser and emitted frequencies, respectively.

$$I_{RF}(\nu_l,\nu_s) \propto P_i \sum_e \frac{2\hat{\Gamma}_{ei}}{\gamma_e} \frac{|\langle i|r_l|e\rangle|^2}{[(\nu_{ei} - \nu_l)^2 + \Gamma_{ei}^2]} \times \left(\frac{|\langle e|r_s|f\rangle|^2 \Gamma_{ef}}{(\nu_{ef} - \nu_s)^2 + \Gamma_{ef}^2} \right) - P_i \sum_{e,e'} \left(\frac{\hat{\Gamma}_{ei}}{\nu_{ee'} + i\Gamma_{ee'}} \right) \times \frac{\langle i|r_l|e\rangle\langle e|r_s^*|f\rangle\langle f|r_s|e'\rangle\langle e'|r_l^*|i\rangle}{(\nu_{ei} - \nu_l + i\Gamma_{ei})(\nu_{e'i} - \nu_l - i\Gamma_{e'i})} \times \left[\frac{1}{\nu_{ef} - \nu_s + i\Gamma_{ef}} + \frac{1}{\nu_{fe'} + \nu_s + i\Gamma_{e'f}} \right] \quad (3)$$

$\langle i|r_{l,s}|e\rangle$ is the i → e transition moment along the space fixed direction of the incident (scattered) electric field polarization vector, ν_{fi} etc. correspond to the frequency spacing between levels f and i, and P_i is the initial population of level *i*.

The key parameters controlling the distribution of RSR into RL and FL features are the relative values of the phenomenological material relaxation rates, Γ, $\hat{\Gamma}$, and γ. Γ_{ab}, the so-called *total* dephasing rate, represents the damping or decay of the phase coherence of the a, b pair of system levels created by the light field interaction(s). Within the framework of the density matrix approach, the phase coherence of these two radiation coupled levels can be destroyed by population (intramolecular) decay, i.e., lifetime effects, or pure-dephasing (intermolecular) interactions, i.e., collisions or solvent fluctuation effects:

$$\Gamma_{ab} = {}^1/_2(\gamma_a + \gamma_b) + \hat{\Gamma}_{ab} \quad (4)$$

γ_a and γ_b are the inverse lifetimes of states a and b and represent the decay rate due to all possible *inelastic* events such as radiative or nonradiative decay, photodissociation, etc. $\hat{\Gamma}_{ab}$ is the environmentally dependent pure-dephasing rate due to *quasi-elastic* events that are not associated with the transfer of population such as quasi-elastic collisions with the solvent. Such events may be viewed as bath-induced fluctuations of the transition energy ν_{ab}. Furthermore, these relaxation rates are directly related to observed vibrational or

electronic line widths. The expressions in the rounded brackets in eqs 2 and 3 represent vibrational and electronic Lorentzian line shapes with half-widths at half-height (HWHH) of Γ_{fi} and Γ_{ef}, respectively.

The observable is I_{RSR}, and the formal partition into components, here given as the sum of three terms (eq 1), is not unique. The separation of RSR exclusively into two positive definite, physically distinct RRS and RF intensities is not possible, in general, due to the I_{mix} term.[14,15] However, the separation given above has the appeal that I_{RRS} corresponds to the standard Kramers–Heisenberg (KH) perturbation theory expression and is characterized by an emission spectrum which has bands at the ground electronic state Raman frequencies ($\nu_s = \nu_l - \nu_{fi}$) and tracks with the excitation wavelength ν_l. The I_{RF} term, in contrast, has an emission spectrum peaked at frequencies corresponding to spacings between (ro)vibronic levels of the excited and ground electronic state ($\nu_s = \nu_{ef}$) and is independent of the excitation wavelength. These are the phenomenological characteristics that define Raman-like and fluorescence-like features, respectively, as discussed above. Furthermore, the RSR partition given in eqs 1–3 emphasizes the crucial role that pure-dephasing plays in controlling the RSR line shape. When the time scale of electronic pure-dephasing is slow compared to electronic lifetime decay, i.e., $\hat{\Gamma}_{ei} \ll \gamma_e$, I_{RF} and I_{mix} are inconsequential and the RSR is all RRS (see eqs 1–3).

The I_{mix} term, not explicitly given here, is of mixed character in that it contains both Raman ($\nu_s = \nu_l - \nu_{fi}$), and fluorescence ($\nu_s = \nu_{ef}$) resonances.[14,15] This term is not positive definite at all emission frequencies, which underscores how this separation of RSR into RRS and RF does not, in general, correspond to independently observable phenomena. However, the I_{mix} term is generally much weaker than the other components, and is typically of the order of the ratio of a vibrational to electronic line width (Γ_{fi}/Γ_{ef}) at $\nu_s = \nu_l - \nu_{fi}$, and here, as in all treatments of RSR, will be ignored. However, it should be appreciated that the separation of RSR into the sum of I_{RRS} and I_{RF} only is, at least formally, an approximation.

Theoretically, different conclusions are reached concerning the distinction between RR and RF when the molecule is postulated to be a two-level, three-level, or multilevel system or when the Raman line width is neglected. For example, treatments of two-level systems or those which assign the Raman transition a δ function line width have no "mixture" term (I_{mix}), and thus the RSR line shapes can be exactly separated into two positive definite RRS and RF intensities.[4,9,13,16,17] Furthermore, a multilevel (>3-level system) description is necessary in order to capture all possible RSR line shapes and distinctions between RRS and RF.

However, the *key* result common to *all* these theoretical descriptions is that pure-dephasing must be present in order to a observe a redistributed emission feature corresponding to resonance fluorescence. In the absence of pure-dephasing the RSR spectrum is given by I_{RRS} alone, the Kramers–Heisenberg (KH) or "isolated molecule" result.

Equation 1 and the discussion so far have been given with the assumption that the incident radiation is perfectly monochromatic (infinitely narrow bandwidth). However, pure-dephasing may arise from stochastic fluctuations of the incident laser excitation fields (radiation-induced pure-dephasing),[5,18,19,27–29] as well as from material-based pure–dephasing (MPD) mechanisms, i.e., collisions. In other words, solvent-induced electronic energy gap fluctuations for a fixed incident frequency will produce pure-dephasing effects analogous to those due to fluctuations in the incident radiation field itself for a fixed electronic energy gap (*vide infra*).

I. Partition of RSR into RRS and RF: The Effects of Material-Induced Pure-Dephasing

In this section we consider the RSR excited by monochromatic, i.e., perfectly coherent, incident radiation. This corresponds to the commonly encountered situation where the laser bandwidth is narrower than the homogeneous width of the resonant absorption band (Γ_{ei}).

A. Resonant Secondary Radiation of Methyl Iodide: No Pure-Dephasing. The X(A) → B(E) absorption spectrum of methyl iodide vapor (202–190 nm) exhibits only diffuse vibronic absorption features due to the rapid photodissociation to CH_3 and I atoms.[30] A RSR spectrum excited at 201 nm, which is resonant with the electronic origin, is shown in Figure 2. The sample is a stream of N_2 at ambient pressure containing <1% of CH_3I, and the excitation bandwidth is <1 cm^{-1}. This RSR spectrum (Figure 2) is unequivocally a RRS spectrum, i.e., all RL. The phenomenological basis for this assignment is summarized below:

1. The spacing between the laser frequency and the strongest emission feature corresponds to the known ground-state frequency of the totally symmetric ν_2 methyl umbrella mode at 1250 cm^{-1}. As the excitation is tuned, the peak position of this band tracks at constant energy displacement from the excitation frequency.

2. The observed RSR line width is <1.6 cm^{-1} (Figure 2 insert) after the instrumental band pass is deconvolved. If the RSR spectrum was predominately RF in character, this line width would correspond to the electronic dephasing width, Γ_{ef} (as an upper limit). Such a narrow line width would result in a sharply structured absorption spectrum due to rotationally resolvable features. This stands in contrast to the observed diffuse vibrationally resolved X(A) → B(E) spectrum.[30]

3. A best-fit to theory of the observed polarization character of the RSR as a function of excitation wavelength is accomplished only for a RRS treatment of this resonance emission and determines the excited-state lifetime to be 0.5 ± 0.1 ps, corresponding to an electronic homogeneous width, Γ_{ei}, of 5 ± 1 cm^{-1}.[30,31] The polarization of the RL component is a sensitive function of the *total* electronic dephasing rate (Γ_{ei}) when this relaxation time scale falls between that of a vibrational (~50 fs) and that of a rotational period (~5 ps).[30–33]

(28) Zhang, Y. P.; Ziegler, L. D. *J. Chem. Phys.* **1990**, *93*, 8605.
(29) Li, B.; Myers, A. B. *J. Chem. Phys.* **1991**, *94*, 2458.
(30) Wang, P. G.; Ziegler, L. D. *J. Chem. Phys.* **1989**, *90*, 4115; **1991**, *95*, 288.
(31) Ziegler, L. D.; Chung, Y. C.; Wang, P.; Zhang, Y. P. *J. Chem. Phys.* **1989**, *90*, 4125.
(32) Myers, A. B.; Hochstrasser, R. M. *J. Chem. Phys.* **1987**, *87*, 2116.
(33) Li, B.; Myers, A. B. *J. Chem. Phys.* **1988**, *89*, 6658.

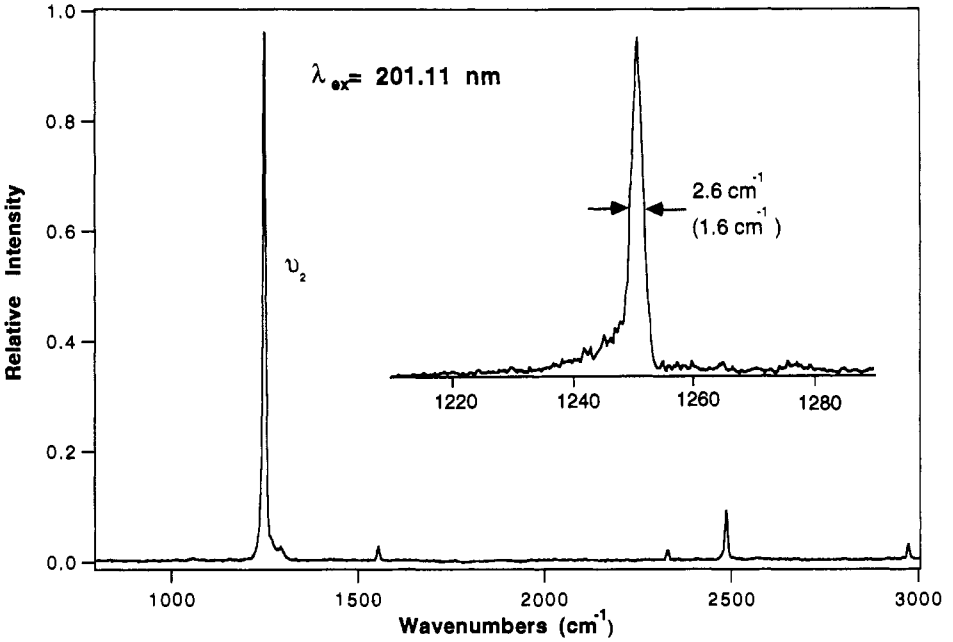

Figure 2. Resonance raman spectrum of CH_3I vapor (ambient) excited at 201.2 nm (bandwidth < 1 cm^{-1}). The inset shows the width of the ν_2 band before (after) deconvolution of the spectral bandpass.

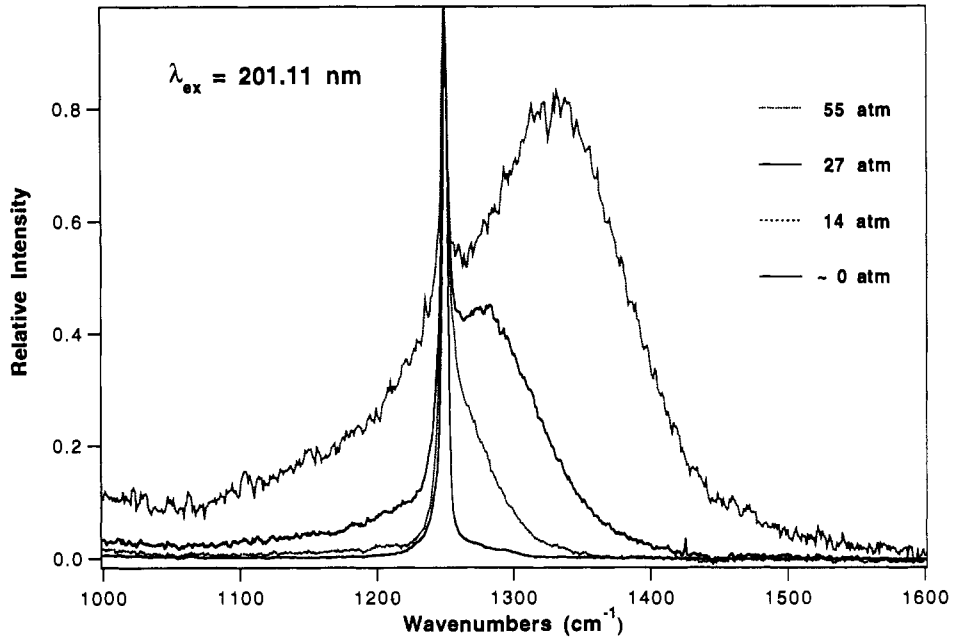

Figure 3. Pressure dependence of the RSR line shape of methyl iodide in methane excited at 201.11 nm.

4. The mean collision time for methyl iodide in 1 atm of N_2 is of the order of 100 ps, which is much slower than the ~0.5-ps lifetime decay due to the excited-state photodecomposition.

These observations establish that this RSR spectrum of methyl iodide vapor is entirely RL. The excited-state lifetime of 0.5 ps is much faster than either material-based ($\hat{\Gamma}_{ei}^{-1} \sim 100$ ps) or radiation-based (~10 ps) pure-dephasing time scales. Consequently, all the spectral features are given by I_{RRS} (eq 2), the KH perturbation result alone (or its Fourier-transformed time-domain equivalent).

B. RSR of Methyl Iodide: The Effects of MPD (Collisions). When methyl iodide vapor is mixed with high pressures of a background gas, the observed RSR line shape becomes more complex and reveals a FL component. The RSR spectra of CH_3I (~5 Torr) mixed with various pressures (0–50 atm) of methane excited at 201 nm is shown in Figure 3. A feature whose width is pressure dependent and broader than the RL bands described above increases relative to the sharp RL feature as the bath (methane) pressure is increased. The narrow RL band continues to track with the excitation wavelength while the broader pressure dependent component remains at a fixed emission wavelength as the excitation is tuned through the B-state absorption band (see Figure 4). These are the phenomenological characteristics which differentiate a RL component from one clearly identifiable as RF. The relative intensity of the FL band to the RL band as a function of material pure-dephasing rate, i.e., methane pressure, increases as $P_{methane}$ increases (see Figure 5). These observations are in agreement with the predictions of theory (eqs 2 and 3).

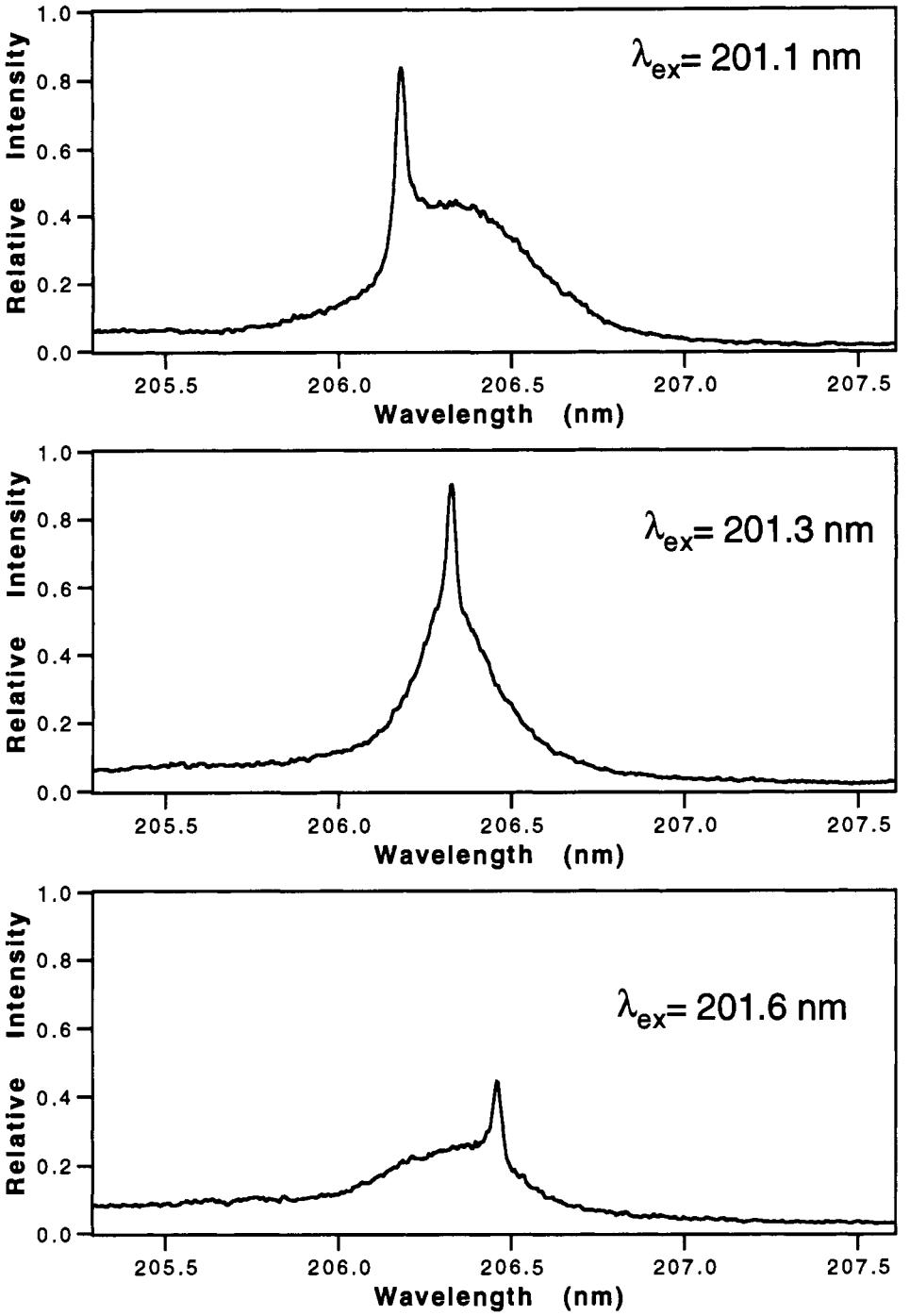

Figure 4. Excitation wavelength dependence of the RL and FL components of the RSR spectrum of methyl iodide in 500 psi (30 atm) of methane. The broad FL feature remains fixed while the narrow RL feature tracks with the excitation frequency.

Furthermore, polarization characteristics also serve to differentiate the pure-dephasing induced component (FL) from the resonance scattering term (RL) as illustrated in Figure 5. The FL band has a depolarization value, ρ (where $\rho = I_\perp/I_\parallel$), which exhibits only a mild pressure dependence, varying from ~0.7 to ~0.8 over the indicated pressure range ($P_{methane} \leq 70$ atm). In contrast, ρ for the narrow RL feature is strongly pressure dependent over the same pressure range and decreases monotonically until reaching an asymptotic value of ~0.12 for methane pressures greater than ~30 atm. The RRS depolarization ratio is dependent on the *total electronic dephasing rate*.[31] Thus as the collision-induced pure-dephasing ($\hat{\Gamma}_{ei}$) contribution to Γ_{ei} increases (increasing $P_{methane}$), the depolarization ratio for the narrow RL band drops from 0.62, its γ_e (isolated molecule or $P_{methane} = 0$) determined value, to 0.125, a limiting symmetry determined value. In contrast, the depolarization ratio of the FL band (see eq 3) depends on the excited-state *lifetime*, γ_e, which remains essentially constant as the methane pressure increases.

These observations demonstrate the crucial role the pure-dephasing time scale, here due to quasi-elastic collisions with the "solvent" (methane) molecules, plays in redistributing RSR into RL and FL components. These emission components are characterized by line widths determined respectively by ground (Γ_{fi}) or excited (Γ_{ef}) electronic state dephasing rates. In the absence of MPD only a RRS term is observed. The FL band intensity and width scales with the pressure (Figure 5 and eq 3) and thus can be used to determine

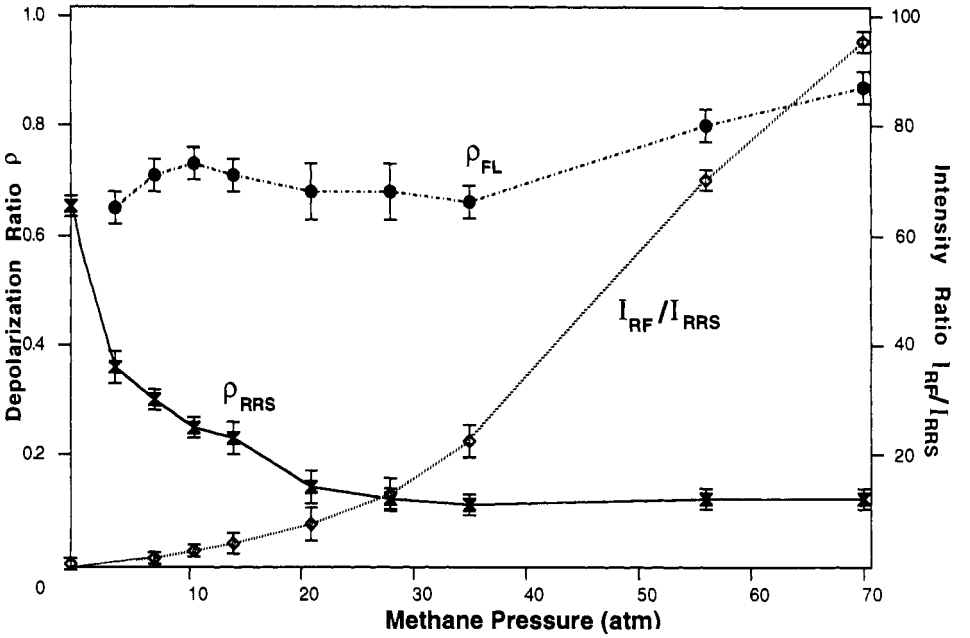

Figure 5. The relative intensities and depolarization ratios ($I_\perp/I_\parallel$) of the RL and FL components of the RSR of methyl iodide vapor as a function of perturbing methane pressure.

pure-dephasing rates.[10,11,13,16,17,22-24] Furthermore, the RL and FL polarization are functions of different excited state relaxation parameters.

II. Partition of RSR into RRS and RF: The Effects of Radiation-Induced Pure-Dephasing

For the CH_3I example discussed above, all the electronic pure-dephasing ($\hat{\Gamma}_{ei}$) is attributed to quasi-elastic collisions, i.e., material-induced pure-dephasing (MPD). However, when the finite bandwidth of the incident radiation approaches that of the molecular resonances of the sample, RSR line shapes may become more complex and the nature of the emission may be altered as a result of the additional dephasing time scales and electronic coherence loss mechanisms introduced by the stochastic phase and amplitude fluctuations of the incident radiation.[19,22,27,28]

In order to demonstrate these radiation-induced pure-dephasing (RPD) effects, we have examined the RSR of O_2 excited both by narrow and by broad band radiation in the region of the Schumann–Runge ($X\ ^3\Sigma_g^- \rightarrow B\ ^3\Sigma_u^-$) absorption system.[28,34] This absorption system consists of a series of weakly absorbing discrete vibrational bands (201–180 nm) which converge to a strongly absorbing continuum region ($\lambda < 175$ nm). Rapid excited-state O_2 photodissociation broadens the discrete rovibrational absorption features (Figure 6).

A. Coherent (Monochromatic) Excitation. A portion of the RSR spectrum of O_2 ($\sim$1 atm) is shown in Figure 7 for two excitation wavelengths, 192.54 and 193.24 nm (bandwidth $\leq$ 1 cm^{-1}), resonant with the overlapped P(7)R(9) and P(17)R(19) rovibronic features of the $X(v=0) \rightarrow B(v'=4)$ absorption band (see Figure 6). Each vibrational transition in these RSR spectra exhibits a triplet rovibrational structure with frequencies corresponding to well-known rovibrational energy spacings of O, Q, S rovibrational Raman transitions on the *ground state* surface. This $\Delta N = 0, \pm 2$ (O, Q, S) structure is due to resonance with the overlapping ΔN = ± 1 (P and R) rovibronic $X \rightarrow B$ absorption bands. When excitation profiles of these rotationally specific RL features are analyzed as resonance Raman intensities, excellent fits to theory are obtained for rovibronic specific homogeneous line widths of $\sim$4 cm^{-1} for the $v' = 4$ B state level.[28] These widths correspond to lifetimes of $\sim$1.2 ps, which are faster than the mean collision time of O_2 at 1 atm and were independent of pressure at experimental conditions (0.5–3 atm). Furthermore, observed ρ values are only consistent with a RRS assignment. Thus, the RSR of O_2 at these experimental conditions is unequivocally RRS.

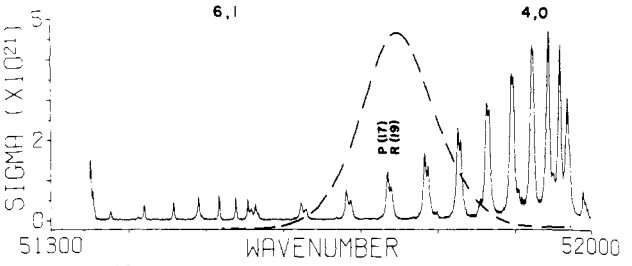

Figure 6. Absorption spectrum of O_2 in the region of the $v' = 4$ band of the Schumann–Runge system. The molar extinction coefficient at the peak of the strongest rovibronic feature is $\sim$3 L mol^{-1} cm^{-1}. The dashed line is the Gaussian spectral density of an ArF excimer laser ($\sim$120 cm^{-1} FWHH).

B. Incoherent (Finite Bandwidth) Excitation. A convenient source of broad band or partially coherent radiation coincident with the Schumann–Runge absorption system is the output of an ArF excimer laser. This radiation has a near Gaussian spectrum with FWHH = 120 cm^{-1} centered at 193.4 nm and overlaps the $v' = 4$ SR absorption band (see Figure 6). The ArF laser excited RSR spectrum of O_2 has a dramatically different and more complex rovibrational band structure than that due to coherent (narrow band) radiation (see Figure 8). The simple O, Q, S triplet Raman structure is no longer observed, and the separations between spectrally resolved emission peaks do not correspond to ground-state rovibrational transition frequencies in the ArF excited spectrum. Instead the

(34) Zhang, Y. P.; Ziegler, L. D. *J. Phys. Chem.* **1989**, *93*, 6665.

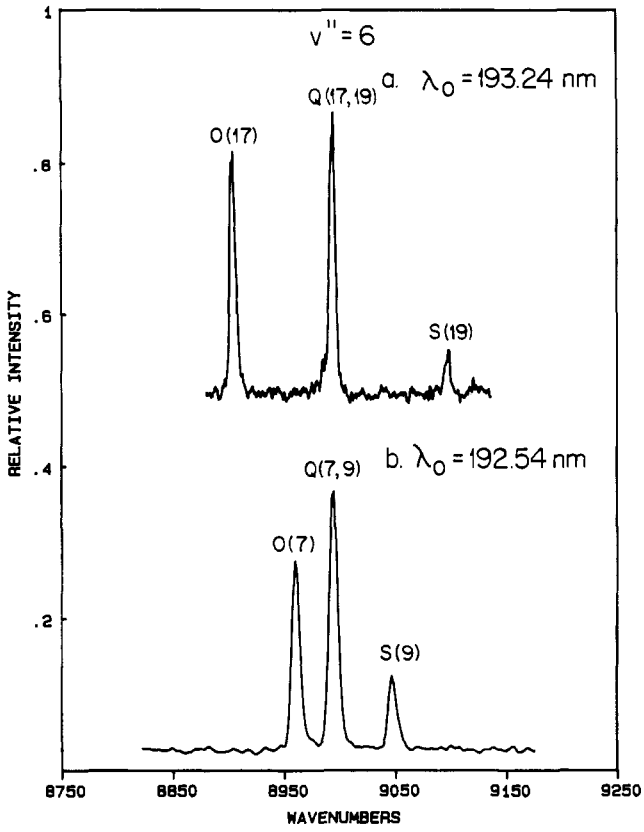

Figure 7. The $v'' = 6$ region of the resonance Raman spectrum of O_2 (1 atm) excited at 192.54 and 193.24 nm with coherent radiation (<1-cm^{-1} bandwidth). Rovibrational Raman assignments are indicated.

observed RSR emission frequencies correspond to $B(v'=4) \rightarrow X(v'')$ P and R rovibronic fluorescence transition energies for emission bands with $v'' > 5$. The nature of the RSR has changed from RRS to RF when the excitation source is changed from narrow (≤ 1 cm^{-1}) to broad band (120 cm^{-1}) with respect to the homogeneous line width of the resonant excited electronic level, Γ_{ei}. This is ~ 4 cm^{-1}, as discussed above, in this region of the SR absorption system. The RF originates from those molecular levels which overlap with the ArF bandwidth (see Figure 6) and have observed RSR line widths of ~ 4 cm^{-1} corresponding to the electronic absorption line width ($\Gamma_{ei} \approx \Gamma_{ef}$). Furthermore, the change from RL to FL character as the incoherence of the excitation is increased is revealed in the polarization as well as the RSR frequencies and band shapes.[28]

In contrast to the unequivocal FL character of the $v'' > 5$ bands in the O_2 RSR spectrum, rich rovibrational structure unlike *either* the RL bands or the FL bands is observed for the $v'' = 2$ to $v'' = 5$ bands (Figure 8). The observed peaks do *not* correspond to energy spacings between rovibrational levels on the ground state (RL) $X(v=0) \rightarrow X(v''=4)$ nor between rovibronic levels of the $B(v'=4) \rightarrow X(v''=4)$ transition (FL). This complex RSR line shape results from interferences between resonant (FL) and near-resonant (RL) electronic sources of RSR cross section due to the RPD effects of the broad ArF excitation.[28] This sign-carrying interference contribution is inconsequential for coherent or narrow band excitation. The relative strengthening of near-resonant terms as the incoherence of the incident radiation is increased occurs because all the Fourier components within the excitation bandwidth contribute to the near-resonant RL component, whereas *only* the resonant Fourier components contribute to the FL component. Hence as the excitation band width is increased, the near-resonant RL contribution to the RSR band shape increases relative to the FL component. Thus, this example highlights that the RSR line shape is in general complex, depends on the time scales of the stochastic interventions, which in this case are due to the excitation fields themselves, and may not be separable into two positive definite RL and FL quantities.

Concluding Remarks

The CH_3I and O_2 resonance emission studies described here unequivocally demonstrate the central role pure-dephasing, i.e., collisions or spectral incoherence, plays in defining RSR as a resonance Raman or resonance fluorescence type of emission. Fluorescence features can only be observed when electronic pure-dephasing rates are as significant as or greater than population decay time scales. These stochastic interactions can arise from either bath (MPD) or radiation fluctuations (RPD). The notion of collision free fluorescence is an oxymoron, unless the excitation bandwidth exceeds the electronic homogeneous width. Once a given spectroscopic basis is chosen, the phenomena presented here illustrate that the notion that this RRS/RF distinction is semantic or just an issue of nomenclature is incorrect.

The phenomenon known as single-vibronic-level (SVL) fluorescence[35] probably deserves more care in the use of this nomenclature and, possibly, in the analysis of the properties of such dispersed spectra. As illustrated here, "SVL fluorescence" is RRS unless the collisional width of the electronic resonance or the excitation bandwidth is greater than that due to lifetime decay of the resonant electronic state. Laser-induced fluorescence (LIF) is another term widely used in experimental physical chemistry that likewise could be used less generically. The nature of the resonance emission as Raman or fluorescence is dependent on experimental conditions. In particular, "LIF" observations of dispersed emission of species in a molecular beam (i.e., collisionless) may be RRS, which could, in principle, affect structural information based on spectral assignments. The ArF excited oxygen spectrum discussed here is an extreme example of such an effect. In fact, it may not be too provocative to state that the ArF-excited RSR spectrum of O_2 is the first unequivocal example of true laser-induced fluorescence, LIF. As demonstrated here, it is clearly the pure-dephasing effects of the excitation laser that induce the fluorescence character to appear.

The correct identification of RSR as RRS or RF must be made in order to properly extract information about chromophore and bath dynamics from these steady state emission observations. Although the RSR discussion has been presented here in the context of

(35) Rordorf, B. F.; Parmenter, C. S. *J. Mol. Spectrosc.* **1978**, *69*, 365.
(36) Heller, E. J. *Acc. Chem. Res.* **1981**, *14*, 368.
(37) Ziegler, L. D. *J. Chem. Phys.* **1987**, *86*, 1703.
(38) Ziegler, L. D.; Chung, Y. C.; Wang, P. G.; Zhang, Y. P. *J. Phys. Chem.* **1990**, *94*, 3394.
(39) Chung, Y. C.; Ziegler, L. D. *J. Chem. Phys.* **1988**, *89*, 4692.
(40) Campbell, D. J.; Ziegler, L. D. *J. Chem. Phys.* **1993**, *98*, 150; *Chem. Phys. Lett.* **1993**, *201*, 159.

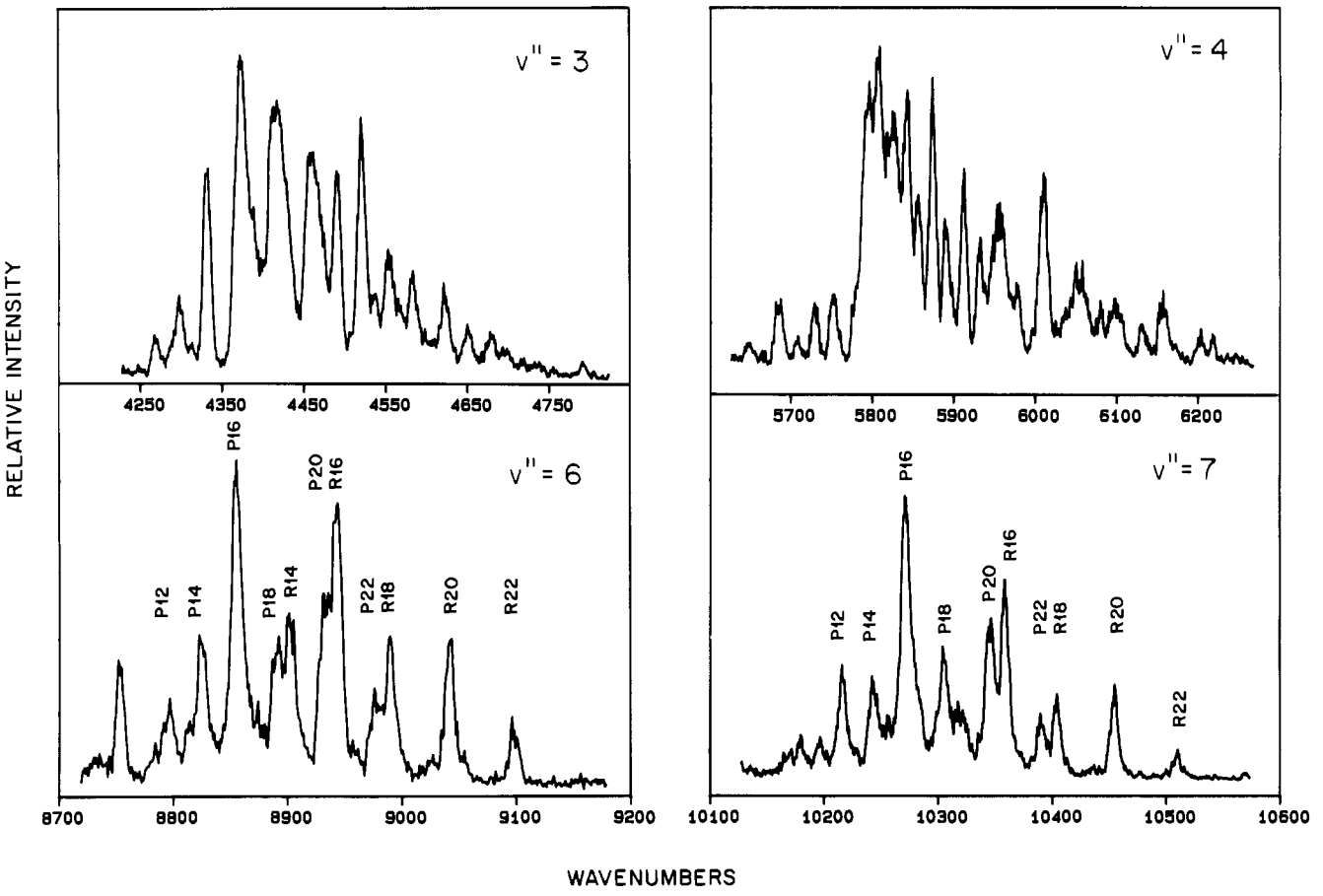

Figure 8. ArF excimer laser (193.4 nm, 120-cm^{-1} bandwidth) excited resonant secondary radiation emission bands of O_2 in regions of $v'' = 3$, 4, 6, and 7. Rovibronic fluorescence assignments are indicated.

frequency domain descriptions, the time domain wavepacket formulations of steady-state RSR emission spectra, which have grown popular during the past decade,[36] must also incorporate all possible dephasing relaxation mechanisms, particularly for condensed-phase studies. The analysis of the RSR of molecules in solutions has proven an effective probe of condensed-phase dynamics.[16,17,20,22-26] Our characterization of the RSR of isolated molecules, clearly a RRS event, allows the quantitative study of ultrafast photodissociation processes with rovibronic specificity.[28,30,31,37-40] Furthermore, turning the emphasis on molecular properties around, the analysis of the RSR of a well-characterized material system can be a measure of the coherence properties of the incident radiation field itself.

I particularly want to thank A. C. Albrecht and P. M. Champion for illuminating and stimulating discussions on this subject over the past several years. I am also indebted to my students and postdoctoral research associates Ronghai Fan, Yun-Po Zhang, Poguang Wang, Deborah Campbell, and Young Chung, whose efforts have contributed to the results summarized here. Our work in this area has been supported by the National Science Foundation and the donors of the Petroleum Research Fund, administered by the American Chemical Society.